Hindawi
International Journal of Antennas and Propagation
Volume 2024, Article ID 3660051, 7 pages
https://doi.org/10.1155/2024/3660051

Research Article

Wireless Pattern Reconfigurable Yagi Antenna Based on Radio Frequency Identification

Chuankui Shen,[1,2] Zhengxing Wang,[3] Liekun Yang,[4] Fengcheng Mei,[5] and Terry Tao Ye[2,4,6]

[1]*Harbin Institute of Technology, Harbin 150001, China*
[2]*Department of Electronic and Electrical Engineering, Southern University of Science and Technology, Shenzhen 518055, China*
[3]*State Key Laboratory of Millimeter Waves, Southeast University, Nanjing 210096, China*
[4]*Southern University of Science and Technology Jiaxing Research Institute, Jiaxing 314031, China*
[5]*College of Big Data and Internet, Shenzhen Technology University, Shenzhen 518118, China*
[6]*Institute of Nanoscience and Applications, Southern University of Science and Technology, Shenzhen 518055, China*

Correspondence should be addressed to Terry Tao Ye; yet@sustech.edu.cn

Received 25 September 2023; Revised 25 January 2024; Accepted 6 February 2024; Published 9 March 2024

Academic Editor: Hervé Aubert

This paper presents, for the first time, the implementation of a pattern reconfigurable Yagi-Uda antenna utilizing radio frequency identification (RFID) technology for remote pattern control. The proposed scheme emphasizes the use of wireless communication instead of long metal cables, resulting in improved stability of the antenna's pattern and return loss. Two low-power consumption single-pole-double-throw (SPDT) switches are employed on a passive resonator, enabling it to function as a director or reflector under the long-range control (up to 25 m) of an RFID reader. Measurement results demonstrate a −10 dB impedance bandwidth of 4.2% and a gain of 7 dBi at 2.41 GHz. The entire system operates with an ultra-low power consumption of 12 μW.

1. Introduction

Pattern reconfigurable antennas have gained considerable attention due to their potential to enhance transmission signal quality and coverage in modern communication systems [1–4]. These antennas can dynamically adjust their radiation patterns to meet specific requirements while operating at a single frequency band. The switching of radiation patterns makes pattern reconfigurable antennas highly desirable for use in a wide range of applications, including cognitive radio, indoor wireless networks, base stations, and multiple-input multiple-output (MIMO) systems [5].

Pattern reconfigurable Yagi antennas typically utilize printed circuit board (PCB) technology and PIN diodes for implementation [1–4]. However, the long direct current (DC) control cables used to maintain the on and off states of the PIN diodes can couple radiation current and significantly impact pattern stability and return loss [6]. In addition, the installation of these antennas in outdoor, rooftop, or base station environments further increases the overall cost of the communication system due to the need for extended control cables.

References [7, 8] present optically controlled and bluetooth-controlled reconfigurable antennas, respectively. However, these methods have limitations such as the high cost and power consumption of optical control and limited control range of Bluetooth. In contrast, reference [9] introduced an RFID wirelessly controlled reconfigurable antenna but only provided simulated results. The RFID-controlled method offers advantages in terms of low power consumption, long control range, and low cost. Commercial RFID tags with −18 dBm sensitivity can achieve communication ranges of tens of meters, and the cost of tags is relatively low. This work represents the first application of RFID technology in the field of smart antenna control, addressing the challenges of long control range and low power consumption. Measurement results demonstrate that our proposed antenna achieves a wireless control range of up to 25 m, while the entire system consumes only 12 μW of power in the common work mode.

This paper starts with an overview of our design, highlighting the problems it aims to solve. The subsequent section provides a detailed description of the antenna's structure, as well as the pattern reconfigurable control circuit. The paper then presents the simulation and measurement results. Finally, a conclusion and discussion are provided in the last part.

2. Proposed Antenna Structure

The proposed antenna is composed of two main parts: the Yagi resonator unit and the RFID tag unit, as illustrated in Figure 1(a). The Yagi resonator unit comprises a rectangular active printed monopole antenna (PMA) resonator and two passive resonators that function as director or reflector elements. Each passive resonator includes two SPDT switches that control the length of the resonator, enabling it to function as a director or reflector. As noted in reference [10], SPDT switches offer superior antenna performance compared to PIN diodes. The control function is executed by the RFID tag, which receives commands from the reader connected to a personal computer (PC). In this section, we provide a detailed description of both the Yagi unit and the RFID unit.

2.1. Yagi Antenna Design. Classic Yagi antennas typically use a dipole structure as the active resonator [3, 11, 12]. However, in modern communication systems, coaxial cable is often used as the transmission line between the antenna and the transceiver, which can cause pattern distortion problem with the differential dipole resonator, resulting in rugged pattern test results [13]. While adding a balun can effectively solve this problem [13], microstrip baluns increase the antenna size, and lumped ferrite and wire baluns induce excessive insertion loss [14]. To address this issue, we use a PMA structure as the active resonator [15, 16], and the size of the PMA is designed following the method in reference [17, 18]. Based on these criteria, the geometry of the proposed Yagi unit is designed in Figure 1(b).

The theory of Yagi antennas, as discussed in reference [12], states that the passive resonator acts as either a reflector or a director based on its effective length compared to the active resonator. When the passive resonator is longer, it exhibits inductive characteristics and functions as the reflector. Conversely, when the passive resonator is shorter, it behaves capacitively and acts as the director. The SPDT switches enable the switching between reflection and direction roles by connecting the center metal patch line to the stub or the open end. The behavior of the SPDT element is controlled by the RFID reader, as shown in Figure 2. The Yagi unit was cosimulated using the electromagnetic and circuit methods with the S3P file [19, 20] in Ansys^{TM} HFSS full-wave simulation software.

2.2. RFID Antenna Design. Our work primarily focuses on the RFID-controlled pattern reconfigurability of the Yagi antenna. As RFID tag antenna design is a relatively mature technology, we provide only a brief description of the tag antenna structure in this paper. Interested readers can refer to books like [21] for more detailed information on tag antenna design.

Two ultra-high frequency (UHF) band RFID tags were implemented on the left and right sides of the Yagi antenna to ensure pattern symmetry. The chosen RFID chip, EM4325, is a low-power consumption Class-3 Generation-2 (Gen2) IC with 4 general input/output (IO) ports. The tag antenna was designed using a folded dipole structure, following the official recommendation in [22, 23], which aims to minimize its impact on the Yagi antenna pattern. The geometry of the folded dipole used in the RFID tag is depicted in Figure 1(b). To simulate the coin battery's effect on the antenna, a circularmetal electrode was incorporated on the backside of the RFID tag, as shown in Figure 1(a). The RFID tag operates in the battery-assisted passive (BAP) mode. One side of the battery provides energy from the EM4325's four general IO ports to the SPDT switches, while the other side improves the tag's sensitivity from −7 dBm to −28 dBm [22].

3. Simulation and Measurement Results

To validate the proposed design, a PCB was designed with the dimensions shown in Figure 1. The substrate material is FR4 ($\varepsilon_r = 4.0 \sim 4.2$, $\tan\delta = 0.012 \sim 0.014$), with a thickness of 1.2 mm. The top and bottom views of the PCB are shown in Figure 3(a).

The antenna's port impedance matching characteristics were assessed through simulated and measured S-parameter analyses, using HFSS and Keysight^{TM} vector network analyzer (VNA) E5071C, respectively. Figure 4(a) presents the simulated and measured S-parameters of the proposed Yagi antenna. It can be observed that the simulated S-parameters for left radiation (state I) and right radiation (state II) are not identical (blue and black lines in Figure 4(a)). This is due to the S-parameter difference between the RF1 and RF2 channels of the SPDT switch [19]. Figures 2 and 1(a) illustrate that the two passive resonators are center symmetric. However, the active resonator is left-right symmetric. Consequently, there is a slight difference in the current distribution of the passive resonators between State I and State II, which can influence the agreement of the S_{11} simulations.

The simulated and measured −10 dB impedance bandwidth could cover the frequency range of 2.36 ~ 2.46 GHz. Simulation and measurement differences are mainly due to manufacturing tolerances such as the dielectric constant, which ranges from 4.0 to 4.2. Furthermore, the SPDT chip was manually mounted on the PCB board using surface-mount technology (SMT) and reflow soldering, leading to the inevitable coupling of the SPDT pads with the passive resonator via parasitic capacitors and inductance.

To demonstrate the antenna's operation property at the measured center frequency of 2.41 GHz, we conducted

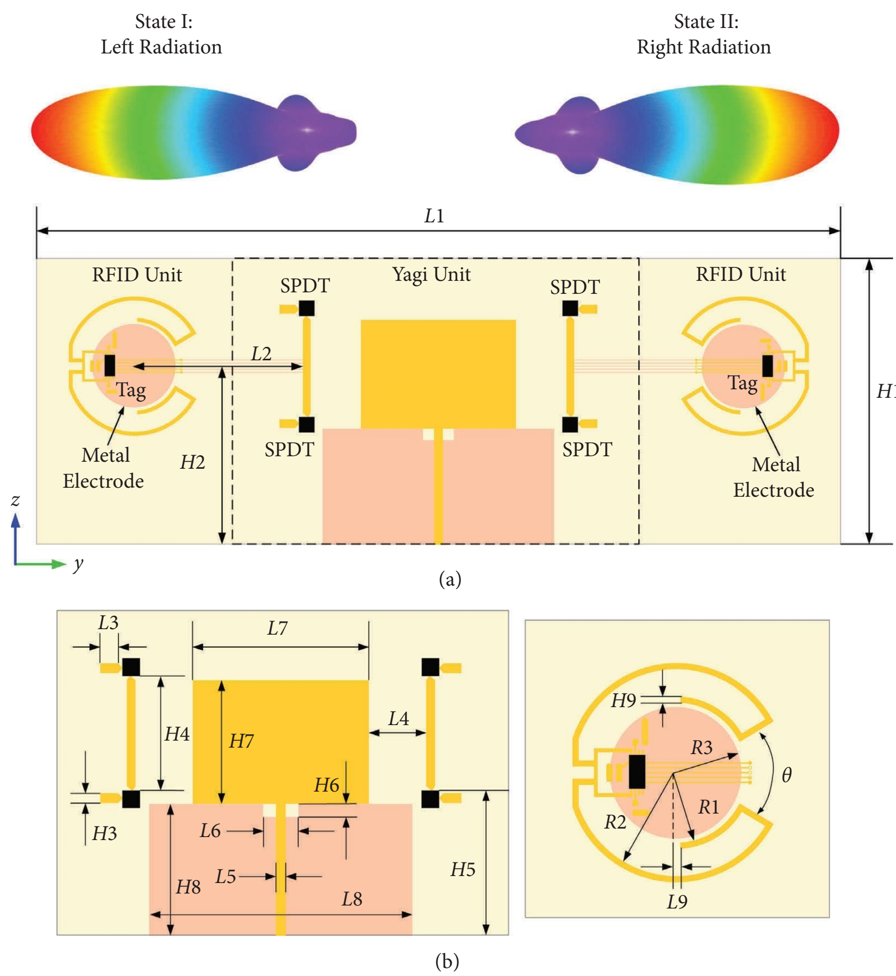

Figure 1: (a) Proposed structure and functionality of the antenna; (b) geometry of the antenna. $L1 = 200$, $H1 = 75$, $L2 = 43$, $H2 = 46$, $L3 = 5$, $H3 = 2$, $L4 = 14$, $H4 = 26$, $L5 = 2.2$, $H5 = 33$, $L6 = 8$, $H6 = 3$, $L7 = 28$, $H7 = 40$, $L8 = 30$, $H8 = 60$, $L9 = 2.5$, $H9 = 1$, $R1 = 12.5$, $R2 = 18$, $R3 = 9.5$, all units in mm. $\theta = 31^{\circ}$.

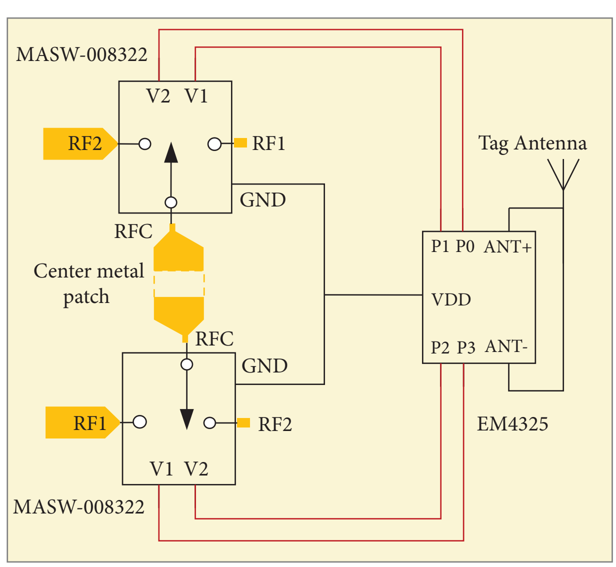

Figure 2: Equivalent control circuit of the SPDT switch.

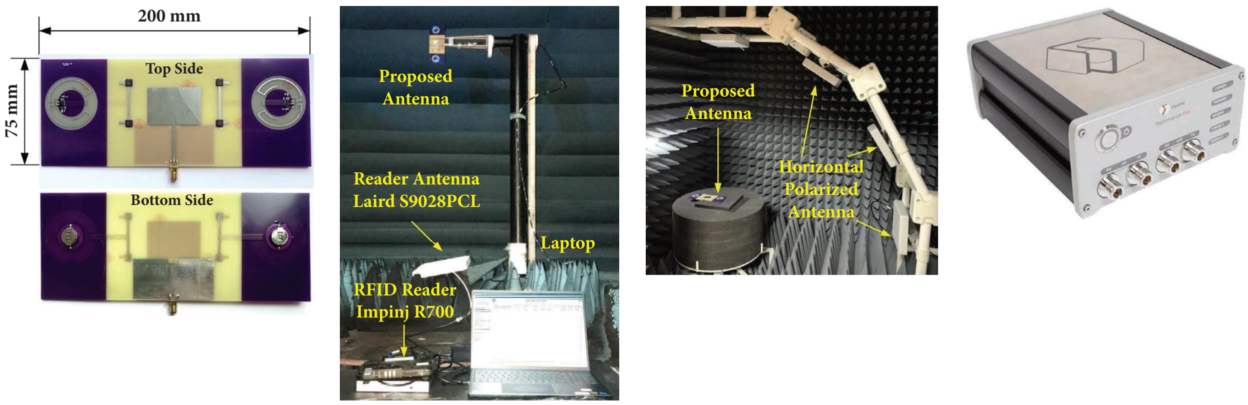

(a) (b) (c) (d)

FIGURE 3: (a) Photograph of the proposed antenna; (b) Yagi antenna measurement environment; (c) RFID tag antenna measurement environment; (d) RFID tag antenna measurement equipment.

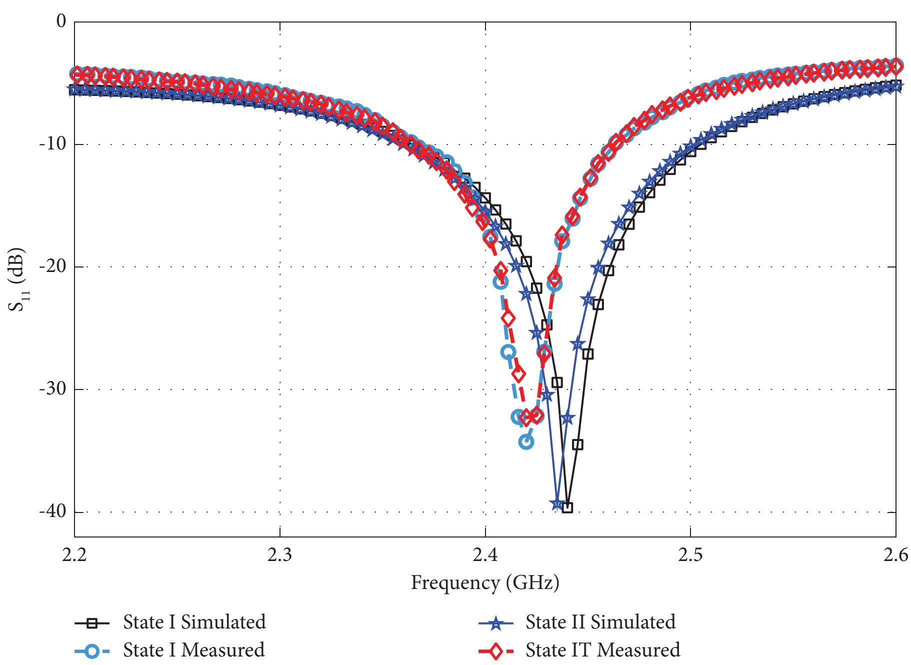

(a)

FIGURE 4: Continued.

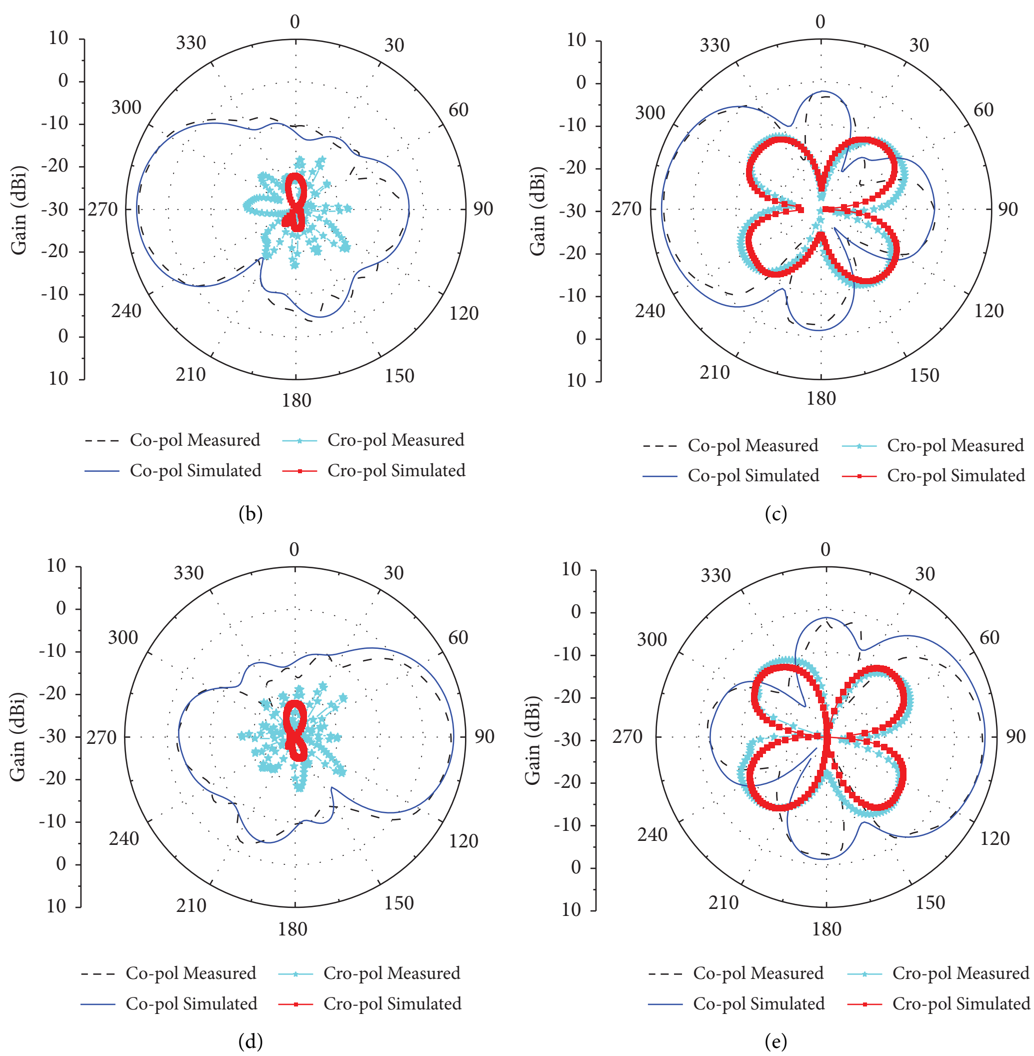

Figure 4: Simulation and measurement results of the Yagi antenna: (a) input reflection coefficient; (b) $E(yz)$-plane in state I; (c) $H(xy)$-plane in state I; (d) $E(yz)$-plane in state II; (e) $H(xy)$-plane in state II.

simulations and measurements of the antenna's electrical field for both states I and II, as depicted in Figure 1(a). The radiation patterns were measured in a professional microwave anechoic chamber, as shown in Figure 3(b).

Figures 4(b)–4(e) present the radiation patterns obtained from both measurement and simulation for the two directional radiation states. Our analysis revealed that states I and II have similar radiation patterns, and the results from both simulation and experiment agreed well. The discrepancies in the radiation patterns can be attributed to various measurement accessories such as the cables, packaged components, and SMA connectors in close proximity to the antenna. We achieved peak gains of 7 dBi and a front-to-back ratio of 10 dB, and the measured radiation efficiencies exceeded 59% for both states at 2.41 GHz.

In Figures 5(a) and 5(b), the simulated port impedance matching characteristics of the RFID tag antenna are shown, which reveal an impedance of $7.1 + j114.2\ \Omega$ at 915 MHz. Since the port impedance of the EM4325 varies at different frequencies, measuring the S_{11} of the tag antenna may have less significance than directly measuring the tag's read range. Following the industrial standard, we measured the pattern and read range of the tag antenna in a semianechoic chamber using professional equipment from Voyantic™ [24] (Figures 3(c) and 3(d)). The performance of the antenna was evaluated using a horizontally polarized antenna with a gain of 6 dBiL. The transmitting power was set to 33 dBm, and the reader sensitivity was −90 dBm. Normalized radiation pattern of the tag antenna is presented in Figure 5(c).

Our implemented antenna has a much higher radiation efficiency (61.6%) than the official recommended design (13.7%). Furthermore, we present the measured read range and a comparison of the forward power and sensitivity of the RFID tag in Figure 5(d). When the tag was placed in the semianechoic chamber, the read range was measured using horizontal polarized antennas and Tagperformance™ software provided by Voyantic™. From Figure 5(d), we can see that the control range of the antenna is 25 m at 915 MHz.

As a summary, a comparison between our work and related pattern reconfigurable schemes is presented in Table 1.

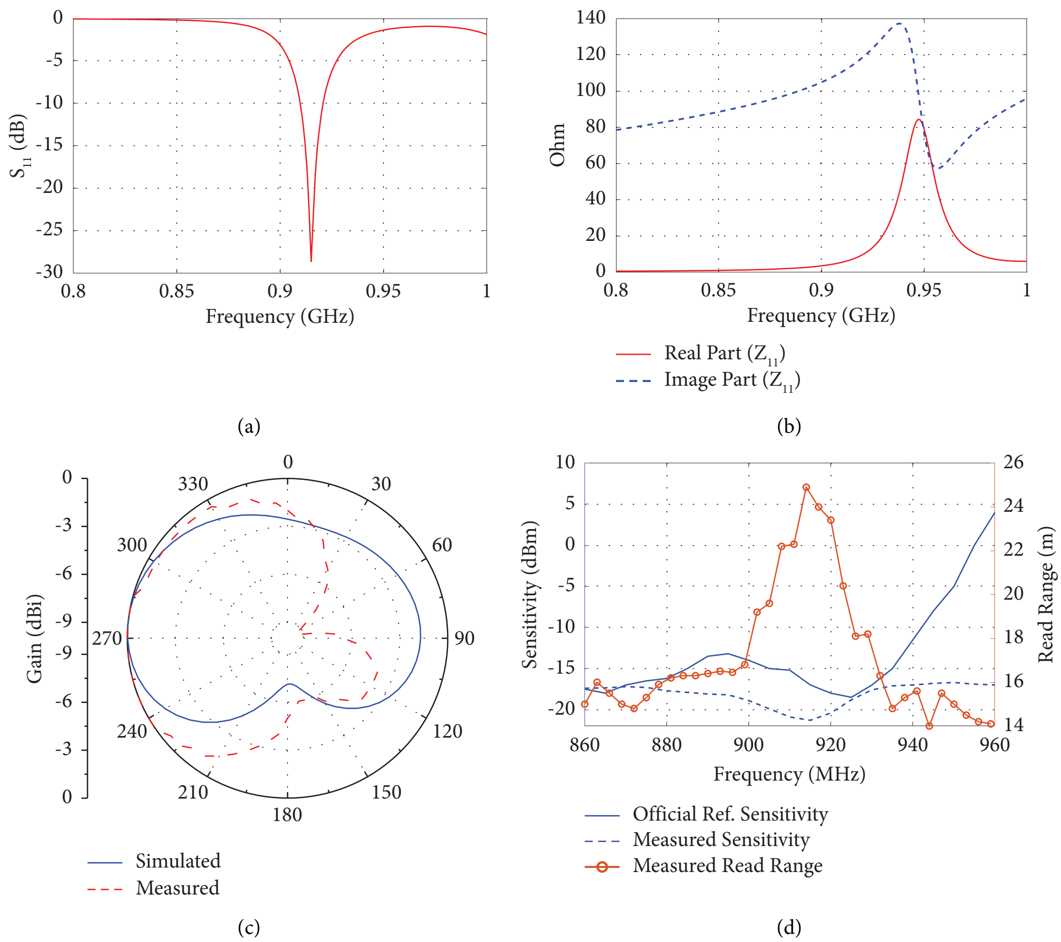

Figure 5: Simulation results of the RFID tag antenna: (a) input reflection coefficient; (b) impedance of the antenna; (c) normalized pattern of the $E(yz)$ plane; (d) read range and forward power on sensitivity of the RFID tag.

Table 1: Reconfiguration schemes comparison.

Ref.	Control mode	Control range (m)	Power consp.	Pattern stability	Cost
[10]	Diodes	>1	>100 mW	No	Middle
[8]	Bluetooth	<10	>10 mW	Yes	Middle
[7]	Laser	>1	>100 mW	Yes	Expensive
This work	RFID	25	12 μW	Yes	Cheap

Conventional pattern reconfigurable methods using diodes and DC control lines suffer from issues related to pattern and return loss stability. When the antenna is built remotely, the consumption of the control cable cannot be ignored. Optically controlled methods can address the pattern stability problem but are limited by the number of antennas that a single laser equipment can serve, as well as their high power consumption and cost. Bluetooth methods, especially Bluetooth low energy (BLE) schemes, have lower power consumption but limited control range, typically not exceeding 10 m. In contrast, RFID technology offers advantages in both power consumption and control range. The cost of RFID readers can be averaged across thousands of tags, making it a feasible option for implementing reconfigurable antenna arrays and phase change array antennas.

4. Conclusion

This paper presents a novel RFID-controlled pattern reconfigurable Yagi antenna designed for wireless communication systems. The antenna operates at a center frequency of 2.41 GHz and achieves a gain of 7 dBi. Measurement results validate the wireless control capability of the antenna at a distance of 25 m, with a power consumption of only 12 μW in the work mode and 36 μW in the dynamic reconfiguration mode. These results confirm the antenna's suitability for remote wireless communication applications, making it a promising candidate for practical use in radio direction finders, digital terrestrial television, cell phone outdoor relays, and other related fields.

Data Availability

No data were used to support the study.

Conflicts of Interest

The authors declare that there are no conflicts of interest regarding the publication of this paper.

Acknowledgments

The Yagi antenna pattern and gain performance was measured by Sporton International INC. (Shenzhen), and the input port performance was measured in the IoT and Microsystems Laboratory of Southern University of Science and Technology. The RFID tag performance was tested in Southern University of Science and Technology Jiaxing Research Institute.

References

[1] S. Gaya, R. Hussain, M. S. Sharawi, and H. Attia, “Pattern reconfigurable Yagi-Uda antenna with seven switchable beams for WiMAX application,” *Microwave and Optical Technology Letters*, vol. 62, no. 3, pp. 1329–1334, 2019.

[2] A. Ghaffar, X. J. Li, W. A. Awan et al., “A flexible and pattern reconfigurable antenna with small dimensions and simple layout for wireless communication systems operating over 1.65–2.51 GHz,” *Electronics*, vol. 10, no. 5, p. 601, 2021.

[3] J. Lu, H. C. Zhang, P. H. He, M. Wang, and T. J. Cui, “Pattern reconfigurable Yagi antenna based on active corrugated stripline,” *IEEE Transactions on Antennas and Propagation*, vol. 71, no. 1, pp. 1011–1016, 2023.

[4] C. X. Mao, L. Zhang, M. Khalily, and P. Xiao, “Single-Pole double-throw filtering switch and its application in pattern reconfigurable antenna,” *IEEE Transactions on Antennas and Propagation*, vol. 70, no. 2, pp. 1581–1586, 2022.

[5] B. Mohamadzade, R. B. V. B. Simorangkir, R. M. Hashmi et al., “A conformal, dynamic pattern-reconfigurable antenna using conductive textile-polymer composite,” *IEEE Transactions on Antennas and Propagation*, vol. 69, no. 10, pp. 6175–6184, 2021.

[6] Y. Nakagawa, N. Michishita, and H. Morishita, “A study on antenna with characteristics of insensitive to metal for installation in proximity to two metal walls,” *Journal of Advanced Simulation In Science And Engineering*, vol. 6, no. 1, pp. 118–127, 2019.

[7] I. F. da Costa, S. A. Cerqueira, D. H. Spadoti, L. G. da Silva, J. A. J. Ribeiro, and S. E. Barbin, “Optically controlled reconfigurable antenna array for mm-wave applications,” *IEEE Antennas and Wireless Propagation Letters*, vol. 16, pp. 2142–2145, 2017.

[8] Y. Tawk, J. Costantine, F. Makhlouf, M. Nassif, L. Geagea, and C. G. Christodoulou, “Wirelessly automated reconfigurable antenna with directional selectivity,” *IEEE Access*, vol. 5, pp. 802–811, 2017.

[9] P. Nikitin, “Wirelessly reconfigurable antenna,” in *Proceedings of the 2015 IEEE International Symposium on Antennas and Propagation & USNC/URSI National Radio Science Meeting*, pp. 2257-2258, Vancouver, Canada, July 2015.

[10] Q. H. Dang, S. J. Chen, and C. Fumeaux, “Utilization of RF-switch ICs and PIN diodes in reconfigurable wearable textile antennas,” *IEEE*, in *Proceedings of the 2022:121-123. Asia-Pacific Microwave Conference (APMC)*, Yokohama, JAPAN, November 2022.

[11] H. Yagi, “Beam transmission of ultra short waves,” *Proceedings of the IRE*, vol. 16, no. 6, pp. 715–740, 1928.

[12] Y. Luo and Q. X. Chu, “A yagi-uda antenna with a stepped-width reflector shorter than the driven element,” *IEEE Antennas and Wireless Propagation Letters*, vol. 15, pp. 564–567, 2016.

[13] J. Hao, J. Ren, X. Du, J. H. Mikkelsen, M. Shen, and Y. Z. Yin, “Pattern-reconfigurable yagi-uda antenna based on liquid metal,” *IEEE Antennas and Wireless Propagation Letters*, vol. 20, no. 4, pp. 587–591, 2021.

[14] P. R. Biggins, *Wideband Balun Design with Ferrite Cores*, California Polytechnic State University, San Luis Obispo, CA, USA, 2014, https://digitalcommons.calpoly.edu/cgi/viewcontent.cgi?article=1282&context=eesp.

[15] J. D. N. Cruz, A. J. R. Serres, A. de Oliveira et al., “Bio-inspired printed monopole antenna applied to partial discharge detection,” *Sensors*, vol. 19, no. 3, p. 628, 2019.

[16] X. Ding and B. Z. Wang, “A novel wideband antenna with reconfigurable broadside and endfire patterns,” *IEEE Antennas and Wireless Propagation Letters*, vol. 12, pp. 995–998, 2013.

[17] A. Martinez-Lozano, C. Blanco-Angulo, H. Garcia-Martinez et al., “UWB-printed rectangular-based monopole antenna for biological tissue analysis,” *Electronics*, vol. 10, no. 3, p. 304, 2021.

[18] C. A. Balanis, *Antenna Theory: Analysis and Design*, John Wiley & Sons, Hoboken, NJ, USA, 2015.

[19] Macom Company, “MASW-008322 GaAs,” 2023, https://www.macom.com/products/product-detail/MASW-008322.

[20] Z. X. Wang, C. K. Shen, J. W. Wu et al., “A long-range and nearly passive RFID-controlled information metasurface,” *Advanced Optical Materials*, vol. 12, 2023.

[21] S. Zuffanelli, *Antenna Design Solutions for RFID Tags Based on Metamaterial-Inspired Resonators and Other Resonant Structures*, Springer, Berlin, Germany, 2017.

[22] E. M. Microelectronic, “EM4325 reference design,” 2023, https://www.emmicroelectronic.com/product/epc-and-uhf-ics/em4325.

[23] D. J. Santos, F. Gomes, and D. M. Santos, “Optimized ultra-low power sensor-enabled RFID data logger for pharmaceutical cold chain,” in *Proceedings of the 2015 IEEE Brasil RFID*, pp. 1–5, Sao Paulo, Brazil, October 2015.

[24] Voyantic, “Voyantic tagformance pro system,” 2023, https://landing.voyantic.com/download-tagformance-pro-catalogue.